Synthesis of iron-rich tri-octahedral clay minerals: A review

Liva Dzene[1, *], Jocelyne Brendle[1], Lionel Limousy[1], Patrick Dutournie[1], Christelle Martin[2] and Nicolas Michau[2]

[1]Institut de Science des Matériaux de Mulhouse CNRS UMR 7361, Université de Haute-Alsace, Université de Strasbourg, 3b rue Alfred Werner, 68093 Mulhouse CEDEX, France

[2]Andra, R&D Division, Materials & Waste packages Department, 1/7 rue Jean Monnet, F-92298 Châtenay-Malabry CEDEX, France

*liva.dzene@uha.fr

Abstract

Examples in materials science and in geology show an interest for iron-rich tri-octahedral clay mineral synthesis in large amounts and with well-defined characteristics. This review summarizes previously reported methods and conditions for iron-rich tri-octahedral clay mineral synthesis. Two approaches of hydrothermal synthesis have been applied: using gel or solid precursors. The most common synthesis approach is the hydrothermal synthesis using gel precursor. The synthesis of 1:1 type clay minerals were performed in reducing conditions in neutral or alkaline pH at various temperature and time ranges. The experimental conditions for 2:1 type clay mineral synthesis were in most cases similar to 1:1 type clay minerals, with in addition acidic pH and oxidizing conditions. The most commonly used methods for identifying and characterizing these minerals are X-ray diffraction, infra-red and Mössbauer spectroscopies as well as transmission electron microscopy. The thermodynamic stability of synthesized phases, as well as the reason for elements adopting a definite configuration and distribution in solid phase remain open questions.

Keywords : greenalite, cronstedtite, hydrothermal synthesis, iron-rich clay minerals, serpentine

1. Introduction

Iron-rich tri-octahedral clay minerals have a high potential as heterogeneous catalyst, e.g. in Fenton-like reactions (Garrido-Ramírez et al., 2010; Li et al., 2015; Wang et al., 2017) and some organic transformations (Arundhathi et al., 2011, 2010; Sreedhar et al., 2009). In nature, these minerals are found in ocean floors, where the serpentinization of olivines occurs (Kodolányi et al., 2012), but such formations are either not easily accessible or not largely abundant. Moreover, natural minerals often contain other mineral phases, which can be considered as impurities for certain applications. To obtain a sufficient amount of pure iron-rich tri-octahedral clay minerals and to study their potential application in catalysis, their synthesis can be foreseen.

Apart for the interest of the application in materials science, clay minerals are also present in deep-geological formations envisaged for CO_2 sequestration or nuclear waste disposal (Bourg, 2015; Grambow, 2016). To predict a long-term stability of these formations, geochemical modelling is often performed, but the lack of thermodynamic data regarding iron-rich tri-octahedral clay minerals places limits to these models. An investigation of the thermodynamic properties of synthetic iron-rich tri-octahedral clay minerals as analogues to naturally formed minerals could provide the missing data. Thus, this could improve our understanding of the long-term stability of these minerals and the respective geological formations in which their natural analogues are present.

The third aspect, where the importance of the presence of iron-rich swelling clay minerals has been suggested is the formation of the first biopolymers on Earth surface (Feuillie et al., 2013; Meunier et al., 2010; Pedreira-Segade et al., 2016). A series of synthetic iron-rich tri-octahedral clay minerals with well-defined characteristics, such as particle size and layer charge could contribute to understanding the adsorption and retention phenomena of these molecules on clay surfaces.

Finally, the presence of iron-rich tri-octahedral clay minerals has been observed on the surface of Mars (Chemtob et al., 2015), in deep-sea sediments (Baldermann et al., 2015; Tosca et al., 2016), during the chloritization (Beaufort et al., 2015) and serpentinization (Kodolányi et al., 2012) in subduction zones and transform faulting, in meteorites (Zolotov, 2015), but the formation conditions remain poorly understood. Their synthesis under well-controlled conditions and parameters could help to understand these phenomena.Previously mentioned examples in materials science and in geology show an interest for iron-rich tri-octahedral clay mineral synthesis in sufficient quantities and with well-defined characteristics. The first report of iron-rich tri-octahedral clay mineral synthesis dates back to 1911 (Van Hise and Leith, 1911), but there has been a growing interest particularly in the latest years (Baldermann et al., 2014; Chemtob et al., 2015; Tosca et al., 2016). Although three general reviews on clay mineral synthesis by Kloprogge et al. (1999), Zhang et al. (2010) and Jaber et al. (2013) exist, as well as a review of Petit et al. (2017) on Fe-rich smectites has been recently published, ferrous iron-rich systems are very particular in terms of synthesis conditions (atmosphere, redox potential) and characterization, making it necessary for a separate review. Three different clay mineral synthesis techniques are known : synthesis from dilute solution, solid-state and hydrothermal synthesis (Carrado et al., 2006). Different variations of hydrothermal synthesis technique have been used to form iron-rich tri-octahedral clay minerals (IRTOCM). They can be divided into two groups based on the type of precursor used: (1) hydrothermal synthesis using gel precursor and (2) hydrothermal synthesis using solid precursor. These two groups are discussed in this review focusing on the initial reactants, conditions, and procedures. This information is then summarized with respect to each mineral type: saponite (2:1 type), serpentine (1:1 type) and chlorite groups. The spectroscopic methods used to characterize iron-rich clay minerals have been previously summarized (Neumann et al., 2011), therefore only brief description of techniques used for IRTOCM identification is mentioned. At the end, the use of IRTOCM in

geochemical simulations and the influence of element speciation in solution on the neoformed phases are discussed.

2. Hydrothermal synthesis based on the use of gel precursor

2.1. Procedure of synthesis

The hydrothermal synthesis method based on the use of gel precursor is the most common to form IRTOCM. A general procedure composed of five steps can be suggested (Figure 1):

1) preparation of a precursor;
2) gel processing;
3) hydrothermal treatment;
4) product processing;
5) storage.

2.1.1. Preparation of a precursor

The synthesis procedure starts with the preparation of a precursor, where an exact known mass of solid compounds or a defined volume of solutions is taken in stoichiometric proportions corresponding to the desired chemical composition of the product. In both cases, whether solid compounds or solutions are used, there are two ways of combining the constituents. In the first case, the order of mixing is the following: (1) metal Fe, Mg or Al salt solutions, (2) source of Si and (3) mineralizing agent (e.g., OH^-). In the second case, the salt solution containing Fe, Mg and/or Al (A) and a solution containing Si and OH^- (B) are mixed separately. Then solution (B) is slowly added to solution (A). After the addition of all the compounds, precipitation of solid phase occurs, often as a gel. A gel is a non-fluid colloidal network containing lamellar or disordered structures that are expanded throughout whole

volume of gel by a fluid (McNaught and Wilkinson, 1997). Less often, precipitated solid phase remains dispersed in the solution in form of suspension. Ideally, the preparation of precursor should result in a homogenous distribution of various elements in the gel matrix (Hamilton and Henderson, 1968), but in practice the formation of clusters of elements can occur. This can generate a heterogeneous distribution of certain elements in the precursor and subsequently the final product can also exhibit some sort of heterogeneity. After the preparation of precursor, depending of the metal source, washing or heating of precipitate can be performed.

2.1.2. Different types of subsequent precursor treatment

Three different approaches can be distinguished for the following synthesis procedure. The first type of approach consists of a gel aging step only. After precipitation of the solid phase, the dispersion is left to age for several weeks or months (Decarreau, 1981; Farmer et al., 1991; Harder, 1978; Tosca et al., 2016). The gel aging step is performed at temperatures ranging from 3 °C to 120 °C. For the second approach, gel aging is followed by hydrothermal treatment (Chemtob et al., 2015; Grauby et al., 1994; Lantenois et al., 2005; Mizutani et al., 1991; Wilkins and Ito, 1967). The hydrothermal treatment step is performed in autoclaves at temperatures from 60 °C to 600 °C over the course of 1 day to 3 months. In the third approach, only hydrothermal treatment is applied (Baldermann et al., 2014; Boukili et al., 2015; Flaschen and Osborn, 1957; Grubb, 1971; Roy and Roy, 1954). Another approach, which was used to obtain the first synthetic clay minerals in laboratory but is no longer in use, consisted of precipitating the solid from dilute solutions at boiling temperature under reflux (Caillère et al., 1953).

A one-step synthesis consisting solely of a gel aging or hydrothermal step have been applied in the studies which focus on the formation conditions of IRTOCM in specific geological environments (Baldermann et al., 2014; Boukili et al., 2015; Chemtob et al., 2015; Decarreau, 1981; Farmer et al., 1991; Flaschen and Osborn, 1957; Grubb, 1971; Harder, 1978; Roy and Roy, 1954; Tosca et al., 2016; Van Hise and Leith, 1911). A two-step synthesis

including both gel-aging and hydrothermal steps has been applied in some cases, where a known and precise material chemical composition is needed (Grauby et al., 1994; Lantenois et al., 2005; Mizutani et al., 1991; Wilkins and Ito, 1967). The heating or washing of sample between the two steps allows removing salts such as nitrates and carbonates so that the precursor's chemical composition corresponds to the one expected for the final product. In practice, the complete washing of anions is impossible in a gel, therefore some deviation from 'ideal composition' should be expected. A one-step procedure consisting solely of hydrothermal treatment could be applied in studies where simple and fast procedure is needed and the presence of impurities can be tolerated.

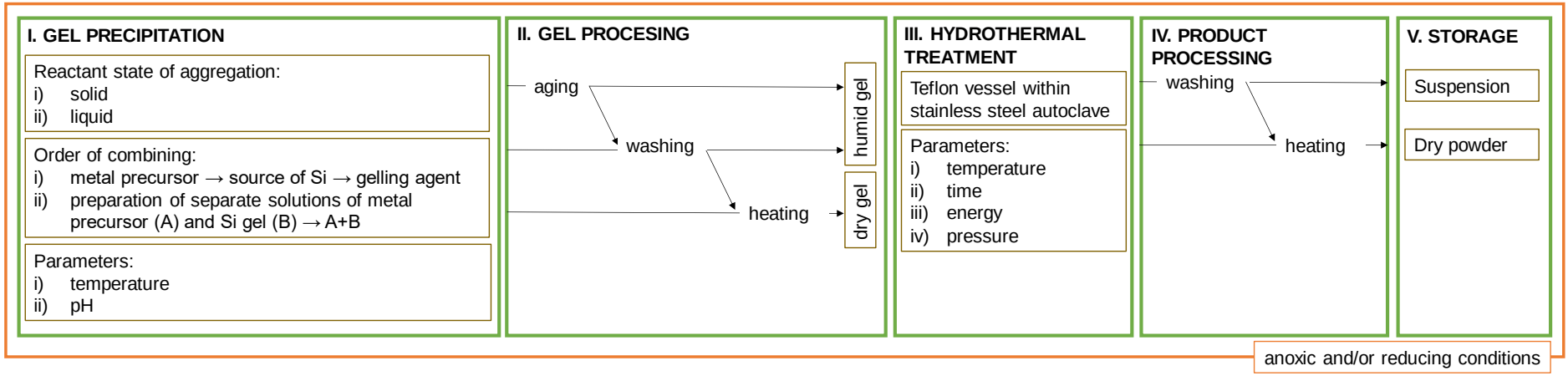

Figure 1. 5-block action scheme detailing the steps of hydrothermal synthesis procedure based on the use of gel precursor for iron-rich trioctahedral clay minerals: (I) gel precipitation, (II) gel processing, (III) hydrothermal treatment, (IV) product processing and (V) sample storage.

2.1.3. Product processing and storage

The processing block includes washing and/or heating of the products. The washing procedure in order to remove the impurities within the neoformed products varies from one synthesis procedure to another, including steps such as centrifugation, filtration and dialysis. The purified synthesis products are then dried either under vacuum or by heating the samples at no more than 120 °C, or freeze-dried. The obtained product is stored as dry powder, except in one case (Baldermann et al., 2014), where it is kept as a dispersion in 6 %wt HNO_3 in order to limit the oxidation of Fe^{2+}. The advantage of storing the solid as a dispersion is the possibility to easily dilute or dry a sample without altering its granulometry. Dispersion of clay minerals particles < 0.2 µm has been observed to be difficult, particularly after drying (Dzene, 2016).

2.2. Synthesis reactants and conditions

2.2.1. Source of silicon

For the synthesis of 1:1 and 2:1 clay minerals, the literature indicates that, tetraethyl orthosilicate (TEOS) $Si(OC_2H_5)_4$ (Boukili et al., 2015; Farmer et al., 1991; Flaschen and Osborn, 1957; Lantenois et al., 2005; Tosca et al., 2016) and sodium silicates ($Na_{2x}SiO_{2+x}$) (Baldermann et al., 2014; Chemtob et al., 2015; Decarreau, 1981; Grauby et al., 1994; Grubb, 1971; Mizutani et al., 1991; Van Hise and Leith, 1911; Wilkins and Ito, 1967) have been identified as excellent sources of Si due to their high solubility in water. One convenience for the use of sodium silicates is the possibility to combine the addition of two elements, i.e., Na and Si, to the reaction mixture with the same reagent. It can be advantageous when looking for reducing total number of steps. However, if there is a necessity to use different Na/Si molar ratios other than can be obtained by sole use of sodium silicates, TEOS can be used as an alternative source. In such a way, it is possible to add an exact amount of Si and also an exact amount of Na with a different reagent. Ethanol, the by-product which forms after the TEOS hydrolysis, can be easily removed by washing or heating.

2.2.2. Source of iron and other metals

For the source of metals (Mg, Al, Fe) and the interlayer cations (e.g., Na^+), the use of different salts such as sulfates, nitrates, chlorides and carbonates has been reported. The type of anion such as sulfates or chlorides has an effect on the subsequent synthesis procedure and on the obtained product (Miyawaki et al., 1991). Four groups of reaction by-products (impurities) which can potentially be formed in the reaction mixture can be distinguished:

1) soluble[1] and having low decomposition temperature <600 °C;
2) soluble and having high decomposition temperature >600 °C;
3) insoluble and having low decomposition temperature <600 °C;
4) insoluble and having high decomposition temperature >600 °C.

These by-products can be removed after precipitation of the gel by washing it with solvent or by heating or after the synthesis by washing with solvent. If soluble salts with low decomposition temperature (<600 °C) such as nitrates NO_3^- are formed in reaction mixture, they can be removed at both stages. Soluble salts with high decomposition temperature (>600 °C) such as sulfates SO_4^{2-} and Li_2CO_3, K_2CO_3, Na_2CO_3 can be removed at both stages, but only by washing. The heating would not be a solution for such salts due to their high decomposition temperature. Insoluble salts with low decomposition temperature such as carbonates (except $CaCO_3$, $BaCO_3$, Li_2CO_3, K_2CO_3, Na_2CO_3) can be removed by heating after the precipitation of gel. Finally, the last group of impurities which can potentially form insoluble products with high decomposition temperature cannot be eliminated by washing or by heating, and thus should not be used in the synthesis. The summary of the impurity characteristics and the way of their removal from the reaction mixture is given in Table 1. Note

[1] Here and hereinafter, the solubility refers to solubility of >1 g/L in aqueous solutions at room conditions.

that the room conditions were considered for the given examples. Different parameters such as pH, temperature, pressure and solution composition can influence the compound solubility.

It has to be considered that during the gel precipitation, the reaction products may become entrained within a hydrogel matrix which contain reactive precursor gel and the impurities, so washing can result in loss of some reaction products as well as truncate formative reaction of products.

The influence of anions on the nature of the synthesis products has not been extensively investigated. Four experiments can be mentioned. Baron (2016) run an experiment comparing the use of $FeCl_2$ and $FeSO_4$ for the preparation of the precursor, which was later used in nontronite synthesis. FTIR spectra of precursors and their synthesis products were identical for both anions used. Thus, in this particular case, when the protocol involved the precipitation of the precursor and its subsequent washing, the anion used to prepare the precursor had minimal effect on the final synthesis product. Also, the synthesis protocol included a control of the pH during the synthesis by an excess of other anions. Therefore, if the pH was not controlled in the synthesis, the anion could influence the final product. Indeed, Miyawaki et al. (1991) notes that sulfate and acetate solutions interfered with the formation of kaolinite more than chlorides and nitrates relating it to the differences in element speciation in solution for these different solution chemistries. The anions present in the solution during the synthesis of beidellite were investigated by Kloprogge et al. (1996). One of the experiments consisted of reacting Si-Al gel at a molar ratio 7.3 : 4.7 with 10 mmol/L salt solution (Na_2CO_3, NaOH, NaCl, NaF) at 350 °C for 10 days at 1 kbar. For samples containing NaCl and Na_2CO_3 salt solutions pyrophyllite was reported as main clay mineral phase. For samples containing NaOH, beidellite was reported, and for sample containing NaF both beidellite and pyrophillite were reported as products. Differences in product formation were attributed to the large impact that the different electrolyte solutions had on the initial pH, which in turn have influence on the final synthesis product.

Finally the fourth study by Huve (1992), which discussed the effect of anion on the resulting product, emphasizes the presence of F^- in the reaction medium and its ability to form complexes with metals. Indeed, F^- can play a role on resulting metal complex solubility and element coordination state, which in turn can influence further the crystallization of solid phases. Clay minerals synthesized using F^- generally show a higher degree of crystallinity compared to other anion salts.

Table 1. Summary of impurity properties and the general ease to remove them (✓) or not (✗) at two different synthesis procedure steps by two different methods.

Impurity properties	Soluble Low decomposition temperature <600 °C	Soluble High decomposition temperature >600 °C	Insoluble Low decomposition temperature <600 °C	Insoluble High decomposition temperature >600 °C
Example	NO_3^-	SO_4^{2-} (except Ca, Ba, As, Pb); Cl^-, K_2CO_3, Li_2CO_3, Na_2CO_3	CO_3^{2-}(except K^+, Li^+, Na^+, Ca^{2+} and Ba^{2+})	$CaSO_4$, $BaSO_4$, $CaCO_3$, $BaCO_3$
Removal after gel precipitation	✓	✓	✓	✗
Removal after synthesis	✓	✓	✓/✗	✗
Removal by heating	✓	✗	✓	✗
Removal by washing	✓	✓	✗	✗

2.2.3. Solution pH during the synthesis

The pH conditions of precursor gel or solution that have been reported, range from neutral to basic (i.e., from 7 to 10) (Table 2 and 3). Most often the initial pH of the prepared reaction mixture was near pH of 8. The adjustment of pH to a specific value is not systematic because of the buffering due to formation of the gel precursors. In the studies where it was carried out, NaOH or NH_4OH solutions at various concentrations were used, except in the study

of Farmer et al. (1991), where $Ca(OH)_2$ was used instead. In the study of Mizutani et al. (1991), a 5M NaOH solution was used to set OH^-/Fe molar ratio to 7, rather than to adjust the initial pH to a specific value. The solution pH affects the solubility of solid compounds, the formation of hydrous gels, and element speciation and activity in the reactive solution. For example, Doelsch et al. (2001) who studied speciation and crystal chemistry of Fe(III) chloride hydrolyzed in the presence of SiO_4^{4-} found that Si-O-Fe bond is present for samples with $Si/Fe \leq 1$ for the range of pH investigated, but absent for samples prepared at pH = 3 for Si/Fe = 2 and Si/Fe = 4 and at pH = 5 for Si/Fe = 4. The role of pH on the synthesis of clay minerals was studied by Baron et al. (2016) and de Kimpe et al. (1961) suggesting that it influences element speciation in the prepared reaction mixture, which in turn influences the product obtained during the synthesis. Baron et al. (2016) reported that the increase in synthesis pH induced the increase of the concentration of anionic aqueous Si species (i.e., $H_3SiO_{4(aq)}^-$ and $H_2SiO_{4(aq)}^{2-}$) in the initial solution, and favored the incorporation of Fe(III) in tetrahedral sites of synthesized nontronites. Frank-Kamenetzkij et al. (1973) pointed out the effect of initial Al coordination on the newly formed clay minerals. As such, the aging of Al-Si gels under constant hydrothermal conditions (450 °C, pH_2O = 1000 $kg \cdot cm^{-2}$, 3 days), but at different pH, resulted in the formation of strongly different phases. In acid solutions, pyrophyllite with octahedrally coordinated Al^{VI}, hydralsite- and andalusite-like phases were formed. In neutral pH, the main newly formed solid was a random mixed-layer phase of pyrophyllite-beidellite type with both tetrahedrally and octahedrally coordinated aluminium (Al^{IV}+Al^{VI}) and hydralsite (Al^{VI}). In alkaline solution, aluminosilicates nepheline, cancrinite, nosean were formed, possessing only Al^{IV}. The study of Fialips et al. (2000) also reported the effect of pH on synthesized kaolinite properties. For acidic pH at the end of synthesis a low-defect kaolinite, with high thermal stability and a hexagonal morphology was obtained, while for the most basic final pH, a high-defect kaolinite, with low thermal stability and lath shape was found.

In practice, pH variation can be important during different synthesis steps, therefore it is important not to forget to measure the solution pH before and after the synthesis, as well as the pH of the solutions used during the experiment. In some cases, the solution pH can be very acidic (close to pH=0) or very basic (close to pH=14), therefore a special care should be taken to choose the most adapted method to measure the pH.

2.2.4. Atmosphere conditions

The experiments of 1:1, and in some cases 2:1, iron-rich tri-octahedral clay mineral synthesis have been carried out under anoxic and/or reducing conditions. Anoxic conditions are ensured in working in glove box under N_2 or Ar atmosphere, and reducing conditions are achieved by adding reducing agents such as sodium dithionite $Na_2S_2O_4$ or hydrazine N_2H_4 solutions. In the study of Decarreau (1981) the presence of oxygen was limited by bubbling pure H_2 through the reaction mixture during all synthesis procedure. The reducing and anoxic conditions ensure that iron is maintained as Fe^{2+} during the experiment as it easily oxidizes in the presence of O_2. Such conditions are necessary to mimic specific environments (e.g., marine environment or Mars atmosphere). Other particular conditions during the preparation of reaction mixture include sea water matrix (Tosca et al., 2016) and addition of F^- (Boukili et al., 2015).

2.2.5. Synthesis temperature and time

Synthesis temperatures vary from 3 °C to 600 °C and last from one day to 3 years. Temperature, like pH, is expected to influence solubility, activity and speciation of elements in solution. Furthermore, it also could have effect on crystal germination, nucleation and growth (Kloprogge et al., 1999). The study of Baker and Strawn (2014) reported an increased cation ordering in synthetic nontronite samples with increased incubation temperature (up to 150 °C), in agreement with synthesis reported by Andrieux and Petit (2010), which also note temperatures up to 150 °C and high pH (around 12) being suitable for the formation of the Fe^{3+}-

rich smectitic end-member (nontronite). Furthermore, they report that higher temperatures (200 °C) and lower pH (down to 7) are suitable for the more Al-rich smectites (Fe^{3+}-beidellites). Regarding the influence of time, Grubb (1971) reports that for the same temperature 2:1 type phase, minnesotaite, becomes dominant over 1:1 type phase for 3-year experiment, while for the same time minnesotaite is dominant at higher temperatures over 150°C compared to greenalite.

The reactants as well as synthesis conditions (pH, temperature, crystallization times) and the obtained phases are summarized in Tables 2 and 3. The names of formed IRTOCM phases have been included as given by the authors.

Table 2. Summary of 1:1 iron-rich tri-octahedral clay mineral synthesis by hydrothermal method using a gel precursor showing the experimental conditions (pH, temperature, aging times) and the neoformed phases.

Publication	Precursor preparation					Aging		Synthesis		Products
	Si source	Fe source	Mg source	pH	Other conditions	Temp., °C	Time	Temp., °C	Time	
Van Hise and Leith (1911)	$Na_2O{\cdot}3SiO_2$	$FeSO_4$ or $FeCl_2$	soluble Mg^{2+} salt	neutral or slightly alkaline	absence of oxygen	-	-	100	n.d.	greenalite
Flaschen and Osborn (1957)	$Si(OC_2H_5)_4$	$FeCl_2$	-	n.d.	very low oxygen partial pressure	-	-	220 to 470	4 to 14 days	greenalite
Grubb (1971)	4% silica sol prepared from dilute sodium silicate solution	$FeCl_2{\cdot}4H_2O$	$MgCl_2{\cdot}6H_2O$	5-8	addition of seeding material (magnetite, kaolinite, montmorillonite, albite, quartz)			110-450	2 days to 3 years	crocidolite, greenalite, minnesotaite
Harder (1978)	H_4SiO_4	$FeSO_4$	$Mg(OH)_2$	pH=7-9 (with NaOH)	N_2 atm.; 0.1% $Na_2S_2O_4$ and 0.1% $N_2H_4{\cdot}2HCl$			3 and 20	more than 1 day	greenalite and chamosite
Mizutani et al. (1991)	$Na_4SiO_4{\cdot}H_2O$	$FeSO_4{\cdot}7H_2O$		pH=3 (with 0.5M H_2SO_4) OH-/Fe=7 (with 5M NaOH)	$Na_2S_2O_4$	room	1 day	150	50 hours	1:1 iron phyllosilicates
Tosca et al. (2016)	$Si(OC_2H_5)_4$	$(NH_4)_2Fe^{2+}(SO_4)_2{\cdot}6H_2O$	-	pH=7; 7.5; 8 (0.1 mM NaOH)	anoxic N_2/H_2 atm.; seawater matrix	-	-	25	~3 months	greenalite

Table 3. Summary of 2:1 iron-rich tri-octahedral clay mineral synthesis by hydrothermal method using a gel precursor indicating experimental conditions (pH, temperature, aging times) and the neoformed phases.

Publication	Preparation of the precursor					Aging		Synthesis		Products
	Si source	Fe source	Mg source	pH	Other	Temp., °C	Time	Temp., °C	Time	
Caillère et al. (1953)	SiO_4^{4-}	Fe^{3+} and Fe^{2+} salts	Mg^{2+} salts	pH=7-9.5 (with NaOH)	HCl, NaCl and KCl	-	-	100	up to 40 days	saponite-like and swelling chlorite-like ferrous phyllosilicates
Roy and Roy (1954)	K_4SiO_4	$FeNH_4SO_4$	-	n.d.	-	-	-	300 and 350	up to two weeks	mica-type phase (Fe^{3+} muscovite)
Wilkins and Ito (1967)	Na_4SiO_4	$FeCO_3$	$Mg(OH)_2$	pH=8 (with conc. NH_4OH)	-	120	n.d.	500-550	15-72 hours	talc $Mg_{52}Fe_{48}$
Decarreau (1981)	$SiO_2{\cdot}Na_2O$	$FeCl_2$	$MgCl_2$	not adjusted	pure H_2 bubbled through during all synthesis, HCl	-	-	25 and 75	15 days	stevensites and saponites
Farmer et al. (1991)	$Si(OC_2H_5)_4$	$FeCl_2$	-	pH=8 (with $Ca(OH)_2$)	1mM N_2H_4, N_2 atm, $CaCO_3$	-	-	23 and 89	8 and 12 weeks	saponite and mixed layer saponite-chlorite
Grauby et al. (1994)	$Na_2O{\cdot}SiO_2{\cdot}5H_2O$	$FeCl_3{\cdot}6H_2O$	$MgCl_2{\cdot}6H_2O$	pH=9-10 (not adjusted)	-	60	12 hours	200	30 days	nontronite - saponite series
Lantenois et al. (2005)	$Si(OC_2H_5)_4$	$Fe(NO_3)_3{\cdot}9H_2O$	$Mg(NO_3)_2{\cdot}6H_2O$	pH=6 (with NH_4OH)	Na_2CO_3, ethanol	80	24 hours	400	1 month	SapFe08
Baldermann et al. (2014)	Na_4SiO_4	$FeSO_4{\cdot}6H_2O$	$MgCl_2{\cdot}6H_2O$	pH=8.5 (with NaOH)	$Na_2S_2O_4$	-	-	60 and 120, and 180	2 and 5, and 7 days	ferrous saponite
Chemtob et al. (2015)	Na_4SiO_4	$FeCl_2$	$MgCl_2$ and $AlCl_3$	pH=8-9 (not adjusted)	N_2 atm	n.d.	overnight	200	15 days	ferrous smectite
Boukili et al. (2015)	$Si(OC_2H_5)_4$	50% as NO_3^- and 50% as metallic Fe	-	n.d.	$Na_2CO_{3\,(s)}$, AlF_3 or FeF_2	-	-	600	7 days	trioctahedral micas

2.2.6. Microwave-assisted hydrothermal synthesis

There has been recently reported the use of microwave radiation to synthesize Fe^{3+}-saponites (Trujillano et al., 2009). The method is based on hydrothermal synthesis as described above, but the difference is that the sample is placed in a microwave furnace, where it is submitted to heat and microwave power at the same time. The microwave power applied causes heating of the water faster and more efficiently compared to simple heating. Thus higher temperature and consequently higher pressure inside the reactor can be reached, thus reducing the rate constant of the reaction. Indeed, the reported reaction time of 8 hours is significantly shorter than during the usual hydrothermal synthesis.

3. Hydrothermal synthesis using a solid precursor

The second group of IRTOCM synthesis comprises the synthesis of IRTOCM from a template or a previously prepared solid precursor. The summary of studies of IRTOCM using this synthesis technique is given in Table 4. A large part of the studies included in this section relates to the research done in the context of nuclear waste disposal, where the interaction between iron from metallic components and clay from natural or engineered barriers was investigated. Here, only some publications of these studies reporting the formation of IRTOCM phases are included. An overview of clay mineral and iron interactions in nuclear waste disposal conditions can be found in Lantenois et al. (2005), Mosser-Ruck et al. (2010) and the references herein.

3.1. Solid templates

As a solid precursor for IRTOCM synthesis, FeSi alloy (Flaschen and Osborn, 1957), glass (Bertoldi et al., 2005) or basalt simulant (Peretyazhko et al., 2016) have been used. In the series of studies related to the nuclear waste disposal context, the interaction of Callovo - Oxfordian claystone (COx) with iron is investigated (de Combarieu et al., 2007; Le Pape et al.,

311 2015; Pignatelli et al., 2014; Rivard et al., 2015). COx is mainly composed of clay minerals
312 (illite, interstratified illite-smectite, chlorite, and kaolinite), with the remaining fraction
313 consisting of silicates (quartz, K-feldspar, plagioclase, and mica), carbonates (calcite, dolomite,
314 siderite, and ankerite), pyrite, sulfates, phosphates, and organic matter (Rivard et al., 2015).
315 Other experimental systems containing solely reference clay minerals such as Wyoming
316 bentonites (MX80 and Swy-2), natural beidellite (Sbld), nontronite (Garfield) (Herbert et al.,
317 2016; Lanson et al., 2012; Mosser-Ruck et al., 2016) and kaolinite (KGa-2) (Rivard et al., 2013)
318 or local bentonites from Slovakia (Osacký et al., 2013) have also been investigated.

Table 4. Summary of iron-rich 1:1 and 2:1 tri-octahedral clay mineral synthesis by hydrothermal technique using a solid precursor including experimental conditions (pH, temperature, aging times) and the neoformed phases.

Publication	Solid	Fe source	Other	Temp., °C	Time	Products
						1 :1
Flaschen and Osborn (1957)	FeSi alloy		very low oxygen partial pressure	220 to 470	4 to 14 days	greenalite
Bertoldi et al. (2005)	glass $3FeO{\cdot}Al_2O_3{\cdot}3SiO_2$			575	90 to 214 days	berthierine
de Combarieu et al. (2007)	Callovo–Oxfordian claystone	powdered iron	inert atm.	90	1 to 6 months	Fe-rich silicate from the serpentine group or chlorite
Lanson et al. (2012)	SbId, Swy-2, Garfield nontronite	metallic Fe powder	Ar atm. ; $FeSO_4$	80	45 days	Fe-rich serpentines (cronstedtite, odinite)
Osacký et al. (2013)	Bentonites	metallic Fe powder	under air atmosphere	75	35 days	7-Å Fe-phyllosilicate
Rivard et al. (2013)	KGa-2	metallic Fe powder	anoxic atm.; NaCl and $CaCl_2$ solutions	90	9 months	Fe-rich serpentines of berthierine-greenalite-cronstedtite domain
Pignatelli et al. (2014)	Callovo-Oxfordian claystone	plates of metallic iron and iron powder	inert Ar atm.; NaCl and $CaCl_2$ solutions; pH = 6.4 at 25 °C	90	6 months	cronstedtite and greenalite
Le Pape et al. (2015)	Callovo-Oxfordian claystone	Fe(0) foil	anoxic atm.; NaCl and $CaCl_2$ solutions	90	2 months	serpentine 1:1 phyllosilicates
Rivard et al. (2015)	Callovo-Oxfordian claystone	metallic iron	anoxic conditions	90	1,3 and 9 months	serpentine family (odinite, greenalite, berthierine)
						2 :1
Peretyazhko et al. (2016)	Adirondack basalt simulant	$FeCl_2$	N_2 atm.; pH=4 (with acetic acid); $MgCl_2$	200	1 and 7, and 14 days	Fe(II)-rich saponite
Mosser-Ruck et al. (2016)	MX80 bentonite	metallic Fe and magnetite powder, iron plate	inert Ar atm.; NaCl and $CaCl_2$ solutions	300	25 months and 9 years	chlorite like minerals or interstratified minerals containing chlorite layers

3.2. Iron source

In the studies of Flaschen and Osborn (1957) and Bertoldi et al. (2005) iron is directly incorporated in the precursor, e.g., in the ferrosilicon alloy or glass melt, respectively. For the group of studies relating to nuclear waste disposal, iron foil (Le Pape et al., 2015), powder (de Combarieu et al., 2007; Lanson et al., 2012; Osacký et al., 2013; Rivard et al., 2015, 2013) or metallic iron plates together with powder (Mosser-Ruck et al., 2016; Pignatelli et al., 2014) were used. The choice to use iron plates together with powder was due to the fact that the powder allows a control of corrosion rate and iron input in solution, while the plates allow a better characterization of alteration products.

3.3. Synthesis conditions

The synthesis in all cases are performed in closed vessels under anoxic conditions. In some cases, N_2 and Ar gases were used (Lanson et al., 2012; Mosser-Ruck et al., 2016; Peretyazhko et al., 2016; Pignatelli et al., 2014). For the group of studies relating to nuclear waste disposal, the medium containing NaCl and $CaCl_2$ solutions was prepared to approach realistic on-site conditions in terms of expected solution composition. The synthesis temperature was 90 °C (de Combarieu et al., 2007; Herbert et al., 2016; Lanson et al., 2012; Le Pape et al., 2015; Pignatelli et al., 2014; Rivard et al., 2015, 2013) and 300 °C (Mosser-Ruck et al., 2016). For the other studies, the temperature was in the range 200- 600 °C (Bertoldi et al., 2005; Flaschen and Osborn, 1957; Peretyazhko et al., 2016). The time for the aging of the systems is very broad varying from 1 day (Peretyazhko et al., 2016) to 9 years (Mosser-Ruck et al., 2016).

The study of Mosser-Ruck et al. (2010) on the effects of temperature, pH, and iron/clay and liquid/clay ratios in the context of nuclear waste disposal reported that low temperatures (<150ºC) and large liquid/clay ratios and iron/clay ratios seem to favor the crystallization of the

serpentine group minerals instead of Fe-rich trioctahedral smectites or chlorites, the latter being favored by higher temperatures.

4. Comparison of hydrothermal synthesis techniques using gel or solid precursors

As mention researchers in *Handbook of Clay science* (Carrado et al., 2006) “More often than not, the main objective of producing synthetic clay minerals is to obtain pure samples in a short time and at the lowest possible temperature.” Furthermore, ideally the steps should be as less as possible, limiting or simplifying such steps as the preparation of the precursor, its treatment and the treatment of the product. One would equally wish that the amount and the state of aggregation allows an easy manipulation of the substances. Thus, based on data reported in Tables 2, 3 and 4, the choice has been made to compare:

- synthesis time and temperature;
- presence/absence of a precursor;
- number and nature of reactants;
- nature of obtained products.

4.1. Synthesis time and temperature

The both parameters, time and temperature, are closely related as states the equation of Arrhenius:

$$k = Ae^{\frac{-E_a}{RT}} \quad \text{(Eq.1)}$$

where k is the rate constant, T is the absolute temperature, A is the pre-exponential factor, E_a is the activation energy of the reaction and R is the universal gas constant. Thus, for a chemical reaction, the reaction rate constant k increases with the increase of the temperature T and/or with the decrease of the activation energy E_a. For both synthesis approaches, this

relation is observed. Experiments performed at lower temperatures (below 100 °C) lasted longer (several weeks or months) than experiments performed at higher temperatures (above 100 °C), which were run only for several days. As an example, Tosca et al. (2016) observed the formation of poorly crystalline greenalite within several weeks of reaction at 25 °C, while Mizutani et al. (1991) reported the formation of well-crystallized greenalite within two days for the reaction at 150 °C. In the studies employing use of solid precursor, the experiments at 90 °C were run during several months to observe the formation of clay minerals (Rivard et al., 2015), while the experiments performed at 200 °C lasted for 14 days maximum (Peretyazhko et al., 2016). Although the relation of shorter reaction time for higher temperature during the experiment is observed for both synthesis approaches, the overall reaction time using gel precursor is generally less when compared to the use of solid precursor.

4.2. Preparation of precursor

Both approaches require preparation of a precursor. For solid precursor method, the preparation of a ferrosilicon alloy or glass requires mixing the ingredients and melting them at elevated temperature (~1400 °C). The preparation of COx or clay minerals requires minimal effort but clay mineral purification. For gel precursor method, the preparation of an amorphous gel requires mixing of the reagents, followed by washing and drying of the gel. Such preparation is more time and effort consuming, but produces more homogenous precursor mixture (Hamilton and Henderson, 1968). Nevertheless it has to be kept in mind that a certain heterogeneity due to clustering of elements during different precursor preparation procedures can occur.

4.3. Reactants

With gel precursor method, every element is introduced by its own chemical compound, usually in form of salt, whereas in solid precursor method all the necessary elements are

introduced together with one solid (ferrosilicon alloy, glass or clay mineral), thus reducing the number of reactants.

4.4. Synthesized products

The synthesis results vary from one study to another and seem difficult to generalize. Nevertheless, solid precursor experiments include a wide panel of different minerals and the discrimination of various kinds of neoformed clay minerals is not always possible. The experiments using gel precursor also represent different products, but clay minerals remain the main phase and in some cases it is possible to draw conclusions on the exact clay mineral type.

The experiments of IRTOCM synthesis present a wide variety of parameters, which makes the comparison between the hydrothermal synthesis methods with gel or solid precursor challenging. For both methods, the synthesis time is similar (not considering studies related to nuclear waste disposal). The temperature range is also similar, but the synthesis of 1:1 clay minerals by hydrothermal method using gel precursor seems to be achieved at lower temperatures. Both methods include different steps to prepare reactants and precursors, with gel reported to produce homogenous precursor mixture, leading in turn to more homogenous synthesis products.

5. Synthesis conditions and identification of IRTOCM

5.1. 1:1 tri-octahedral clay minerals (serpentine group)

5.1.1. Common features of synthesis conditions

The 1:1 tri-octahedral Fe-rich clay mineral synthesis reported in the literature were performed by hydrothermal method using gel precursor (Table 2). This mineral group has also been reported to form during COx and metallic iron interaction (Table 4). All of these experiments were performed under anoxic atmosphere (Bertoldi et al., 2005; de Combarieu et al., 2007; Flaschen and Osborn, 1957; Lanson et al., 2012; Le Pape et al., 2015; Pignatelli et

al., 2014; Rivard et al., 2015, 2013; Tosca et al., 2016; Van Hise and Leith, 1911) or in reducing conditions using such chemicals as sodium dithionite $Na_2S_2O_4$ (Harder, 1978; Mizutani et al., 1991). The pH for the reported synthesis was neutral to alkaline. The reactants for precursor preparation, synthesis temperature and duration were different from one study to another (discussed previously).

5.1.2. Identification and characterization

The identification of the Fe-rich IRTOCM is a challenging exercise requiring the data from several techniques (Stucki, 2013; Stucki et al., 1989). The main techniques used to characterize synthesis products are X-ray diffraction (XRD), transmission electron microscopy (TEM) and Mössbauer spectroscopy. In some cases, Fourier transform infrared spectroscopy (FTIR) and energy-dispersive X-ray spectroscopy (EDX) coupled to TEM have been used.

The early identification of synthesized phases was based on the comparison of synthesized phases with naturally occurring minerals. Thus, Van Hise and Leith (1911) identified the ferrous silicate precipitate as greenalite comparing the granular structure and optical properties of synthesized product with natural rock photomicrograph images. Later, Flaschen and Osborn (1957) reported the synthesis of greenalite in Fe_xO_y-SiO_2-H_2O system mentioning that the powder XRD pattern corresponds closely to that of natural greenalite, but unfortunately no XRD data were included in the publication. Afterwards, in the case of relatively simple systems, i.e., Si-Fe and Si-Fe-Mg or Si-Fe-Al, powder or oriented XRD patterns showing approximately 7 Å periodic structure allows to classify the synthesis product as Fe-rich 1:1 clay mineral (Bertoldi et al., 2005; Harder, 1978; Mizutani et al., 1991; Tosca et al., 2016). TEM can reveal characteristic hexagonal platelet shape (Mizutani et al., 1991) and HRTEM confirms 7 Å periodicity (Bertoldi et al., 2005). Mössbauer spectroscopy was used to obtain information about Fe^{2+}/Fe^{3+} ratio. In the case of the presence of a majority of Fe^{2+}, tri-octahedral structure is suggested (Bertoldi et al., 2005; Mizutani et al., 1991). Furthermore,

FTIR identification of Fe^{2+}_3-OH bands in middle infra-red region (3625 cm^{-1} stretching and 653 cm^{-1} bending) can support the presence of tri-octahedral character (Fialips et al., 2002; Tosca et al., 2016). In the case of Si-Fe-Al system, 1:1 tri-octahedral clay minerals can be classified as berthierine (Bertoldi et al., 2005).

For more complex systems, where the four main elements are present, i.e. Si-Fe-Al-Mg, the identification and classification are even more difficult. The study of Osacký et al. (2013) have revealed also the interest to use the near infra-red region for the identification of neoformed phases. Thus, a band near 4350 cm^{-1} assigned to both Fe(II)Mg-OH and Fe(II)Fe(II)-OH combination vibrations serves as an additional argument to X-ray diffraction data to prove the formation of new 7-Å Fe-clay mineral phase when changes in middle infra-red region are not so obvious. Moreover, the assignment of the combination vibrations can be improved knowing the positions of the OH stretching and bending bands. For example, Gates (2008) showed, where the bending modes of Fe(II)Fe(II)-OH and Fe(II)Mg-OH reside. With these informations, the combination bands could be better identified and assigned. In the case of the studies related to the interaction of COx with metallic Fe, the early studies of this system (de Combarieu et al., 2007), coupled XRD and scanning electron microscopy (SEM) to conclude that Fe-rich silicate from the serpentine group or chlorite have been formed. Further more detailed studies including the characterization by FTIR, TEM-EDX and Mössbauer spectroscopy revealed the heterogeneity of the newly precipitated phases belonging to 1:1 clay mineral serpentine group odinite-greenalite-berthierine domain (Le Pape et al., 2015; Rivard et al., 2015). A thorough study of materials by X-ray spectroscopy evidences as well the mixture of starting solid phase (kaolinite in this study) and Fe-serpentine layers of berthierine-greenalite-cronstedtite (Rivard et al., 2013). The combined use of TEM-EDS and scanning transmission X-ray microscopy (STXM) results had allowed to quantify the percentage of berthierine and cronstedtite-greenalite type minerals in the analyzed material. For two other

studies, the thorough characterization indicated that the obtained phases fall close to cronstedtite and greenalite (Pignatelli et al., 2014) or cronstedtite and odinite-type minerals (Lanson et al., 2012).

5.2. 2:1 tri-octahedral clay minerals (saponite group)

5.2.1. Common features of synthesis conditions

The 2:1 IRTOCM synthesis was mainly performed by hydrothermal method using a gel precursor (Baldermann et al., 2014; Chemtob et al., 2015; Decarreau, 1981; Farmer et al., 1991; Grauby et al., 1994; Lantenois et al., 2005; Wilkins and Ito, 1967), except the studies of Trujillano et al. (2009), Caillère et al. (1953) and Peretyazhko et al. (2016). Trujillano et al. (2009) had reported the preparation of Fe^{3+}-saponite by hydrothermal synthesis assisted by microwave radiation. Caillère et al. (1953) reported the synthesis of saponite-like and swelling chlorite-like ferrous clay minerals by precipitation of solid at boiling temperature. The occurrence of Fe(II)-rich saponite was reported by Peretyazhko et al. (2016) reacting solid (basalt simulant) with $FeCl_2$ solution. From the series of studies related to the context of nuclear waste disposal, Herbert et al. (2016) had identified different 1:1 and 2:1 tri-octahedral mineral interstratifications such as cronstedtite-saponite-trioctohedral vermiculite, berthierine-saponite and chlorite-saponite-trioctahedral vermiculite among other phases.

To synthesize 2:1 IRTOCM with hydrothermal method using a gel precursor, TEOS or sodium silicate have been used as source of Si (Table 3). The sources of Fe and Mg are various including chlorides, sulfates, nitrates and carbonates. The pH of the solution after the precursor precipitation had been reported to be basic in most cases. Acidic pH has been reported in the study of Lantenois et al. (2005) (pH=6) and Peretyazhko et al. (2016) (pH=4). Some, but not all, studies report using inert or oxygen-poor atmosphere conditions (Chemtob et al., 2015; Decarreau, 1981; Farmer et al., 1991; Peretyazhko et al., 2016). In the study of Baldermann et al. (2014), reducing conditions were ensured by adding sodium dithionite to reactants. The

aging of precursor is not systematic and reported in three cases (Grauby et al., 1994; Lantenois et al., 2005; Wilkins and Ito, 1967) for the temperature range of 60 °C to 120 °C and over durations of 12 to 24 hours. The reported range of synthesis temperatures is large varying from 23 °C to 600 °C (Table 3). The synthesis time of 2:1 IRTOCM was reported from 1 day to 2 months (Table 3), which is though shorter compared to 1:1 IRTOCM synthesis, where experiments are reported to last up to 9 months.

5.2.2. Identification and characterization

Early studies of 2:1 IRTOCM used XRD and FTIR to characterize synthesis products (Caillère et al., 1953; Decarreau, 1981; Farmer et al., 1991; Wilkins and Ito, 1967), but owing to their time the publications included only limited examples of XRD or FTIR spectroscopy experimental data. Fortunately, the subsequent work could benefit accommodating more experimental data in the publications. Routine powder XRD analysis coupled with FTIR spectroscopy allows the identification of type of neoformed clay mineral phase and to check the presence or absence of impurities (Boukili et al., 2015; Chemtob et al., 2015; Grauby et al., 1994; Lantenois et al., 2005; Peretyazhko et al., 2016; Trujillano et al., 2009). Different treatments of oriented preparations of XRD slides (saturation with Ca, K, ethylene glycol and heating to 500 °C) have potential identifying interstratified phases (Farmer et al., 1991). Nevertheless, the XRD along with FTIR spectroscopy both remain bulk analysis for clay mineral structure identification. There could be several reasons for the broadness of diffraction peaks such as the aforementioned interstratification or poor crystallinity. The analysis of separate particles using TEM or high-resolution TEM can bring clarification to these points, but the sample representativeness is largely reduced (Baldermann et al., 2014; Inoué and Kogure, 2016). It can be overcome to some extent with large number of analysis. Recently Chemtob et al. (2015) used X-ray absorption spectroscopy (XAS) methods to provide a supplementary proof of tri-octahedral character of neoformed iron-saponite phases.

The chemical analysis of synthesis products have been determined by electron microprobe analysis (Lantenois et al., 2005; Peretyazhko et al., 2016), inductively coupled plasma optical emission spectrometry (ICP-OES) (Chemtob et al., 2015) and analytical electron microscopy (AEM) (Baldermann et al., 2014; Grauby et al., 1994). In the case of pure clay minerals obtained, bulk sample analysis such as ICP-OES and Mössbauer spectroscopy can be considered to establish sample stoichiometry (Chemtob et al., 2015). On the other hand, single particle analysis can potentially evidence the chemical heterogeneity of sample (Grauby et al., 1994), but require sufficient amount of data to be statistically representative. In the studies, where several crystalline phases where identified, single particle analysis by energy dispersive X-ray spectroscopy (EDX) and electron energy loss spectroscopy (EELS) can be more relevant (Baldermann et al., 2014).

5.3. Chlorites

5.3.1. Common features of synthesis conditions

The synthesis of iron-rich tri-octahedral chlorite (chamosite) has been reported by Harder (1978) and Mosser-Ruck et al. (2016). In both cases, chamosite is reported occurring with other clay minerals, also as an interstratified phase. The synthesis experiments have been described in previous sections. For the series of experiments related to the nuclear waste disposal (Mosser-Ruck et al., 2010) on the effects of temperature, it was found that low temperatures (<150ºC) seem to favor the crystallization of the serpentine group minerals, while higher temperatures favor the formation of Fe-rich trioctahedral smectites or chlorites. Nevertheless, Harder (1978) reported the formation of chlorite in the temperature as low as 20 °C, but as discussed previously the limits to include the experimental data in older publications does not allow the interpretation of data today. In geological systems, different range of temperatures for chlorite formation have been distinguished (Beaufort et al., 2015). Its formation temperature is near 200 °C in hydrothermal systems, but in diagenetic systems Fe

chlorite is reported to form in 40 °C-120 °C range. Such difference was attributed to different heating rates, heat-flow conditions and pressure.

5.3.2. Identification and characterization

The same characterization techniques as described previously for 1:1 and 2:1 clay minerals have been used identifying chamosite. As it often occurs as interstratified phase and has different polytypes, great care has been taken to consider and to study these aspects by XRD (Bailey, 1988; Reynolds et al., 1992) and HRTEM (Inoué and Kogure, 2016).

6. Geochemical simulation using thermodynamic properties of IRTOCM

One of the interests in the study of synthesis or IRTOCM is their incorporation in geochemical simulations in order to predict long-term stability of certain geological formations. Clay minerals have a wide variety of isomorphic substitutions, they occur as mixed-layer phases and have small particle size usually less than 2µm. This structural and chemical complexity makes it difficult to introduce them in such simulations. Nevertheless, several numerical approaches have been developed for the estimation of thermodynamic properties of clay minerals (Chen, 1975; Chermak and Rimstidt, 1989; Nriagu, 1975; Sposito, 1986; Tardy and Fritz, 1981; Tardy and Garrels, 1974; Vieillard, 2000, 1994) and introduced in different databases such as Thermoddem (Blanc et al., 2012) or LLNL (Johnson et al., 2000). These databases are particularly useful when applied in geochemical simulation codes such as PHREEQC (Parkhurst and Appelo, 2013) or Geochemist's Workbench® (Bethke, 2007) among others to simulate various systems.

Three approaches can be distinguished for the estimation of thermodynamic properties of clay minerals. First approach, consists of the summation of respective oxyde and/or hydroxyde parameters using "polyhedral summation" (Chermak and Rimstidt, 1989; Nriagu, 1975; Sposito, 1986; Tardy and Garrels, 1974), "regression" (Chen, 1975) or "electronegativity

differences of cations" (Vieillard, 2000, 1994) techniques. Second approach is based on the ideal mixing of end-member clays (Tardy and Fritz, 1981) and the third approach uses the data of ionic species for the estimation of thermodynamic properties (Eugster and Chou, 1973). The last approach is limited to a particular case, where a direct precipitation of solid from solution occurs. As no direct measurements of IRTOCM thermodynamic properties have been performed, the application of second approach is also limited. Therefore, in studies, where simulations involving IRTOCM were performed, the first approach (summation of oxyde/hydroxyde parameters) has been used (Chevrier et al., 2007; Halevy et al., 2017; Zolotov, 2015), because the thermodynamic properties of oxydes and hydroxydes are rather well known (Snow et al., 2011, 2010a, 2010b; Stølen et al., 1996).

Two recent studies have dealt with the confrontation of the experimentally observed formation of iron-rich tri-octahedral clay minerals and the data issued from geochemical simulation (Pignatelli et al., 2013; Wilson et al., 2015). The experiments performed by Wilson et al. (2015) estimated montmorillonite stability in contact with iron. In this study the polyhedral summation technique of clay mineral constituting oxides and hydroxides were used to obtain their thermodynamic properties (Helgeson et al., 1978; Holland, 1989). The study revealed that experimentally detected phases were in agreement with simulations. Another experiment of Pignatelli et al. (2013) used a database Thermoddem (Blanc et al., 2012) (which includes the approach of Vieillard (2000, 1994) on oxyde summation based on the electronegativity differences of cations). In this study (Pignatelli et al., 2014) the stability field of cronstedtite was calculated and confronted with the data of their experimental observations. They note that below 50°C cronstedtite is predicted to be more stable than what it is observed and this difference was attributed to the various polytypes of mineral which is not taken into account in the calculations of Veillard's approach. Moreover, to explain the presence of several phases instead of one as predicted by geochemical simulations, they suggest a reaction path with local

591 changes in Fe concentration. Two aforementioned experiments deal with rather complex
592 systems, and have allowed to compare the formation of one or several particular mineral phases
593 at given experimental conditions.

594 A recent study of Tosca et al. (2016) focused on single IRTOCM, greenalite, formation
595 conditions by direct precipitation. To compare the obtained mineral thermodynamic properties
596 with the literature, they performed solubility experiment, thus obtaining information about the
597 equilibrium constant of the reaction. The obtained experimental values were compared with the
598 data calculated by Eugster and Chou (1973) and agrees rather well. The difference is attributed
599 to the fact that clays are particles of finite size, while in thermodynamics the assumption is
600 made that the phase is infinite. Important that they note to be in thermodynamic equilibrium
601 conditions, where the formation of other metastable phases can be omitted.

602 Although the experiment of Tosca et al. (2016) was performed at equilibrium
603 conditions, in practice such conditions are difficult to achieve or impossible to demonstrate
604 especially for more complex systems such as in the studies of Wilson et al. (2015) and
605 Pignatelli et al. (2013). Thus, the experiments (unsteady state) performed are compared with
606 calculations obtained from a thermodynamic equilibrium (steady state). Even though, the
607 formation of a mineral or its dissolution can be predicted to occur under given conditions, these
608 processes could be negligible because their rate is very slow. For this reason, kinetic evaluations
609 should be also considered. Recently numerical models involving nucleation and crystal growth
610 have been developed, which take into account the change occurring in the system (time
611 dependence) (Noguera et al., 2006a). Such model can be compared with experimental results
612 because the operating conditions are close to the modelling hypothesis. In perspective, it would
613 be interesting to confront these calculations with experimental observations of the formation of
614 iron-rich tri-octahedral clay minerals.

615 ## 7. Iron (III) and aluminium configuration and distribution

Apart from geochemical simulations, other interest in IRTOCM synthesis lays in the possibility to control the synthesized phases chemistry and structure, which in turn can give information about the formation conditions of such phases in natural environments. Most common elements possible to constitute IRTOCM are Si, Mg, Al and Fe. M(II) such as Mg and Fe(II) and M(IV) such as Si can enter only octahedral and tetrahedral sites in clay mineral structure only, respectively, but M(III) such as Al and Fe(III) can be found in both, in tetrahedral and octahedral sheets in different proportions. Recent studies link this feature to the element speciation in the reactant solution (Baron et al., 2016). Thus, Pokrovski et al. (2003) have shown that in Si-free solution Fe(III) adopts octahedral coordination whereas in the presence of Si, a portion of Fe(III) is found to be tetrahedrally coordinated. The experiments performed by Baron et al. (2016), indeed show an increase of tetrahedrally coordinated Fe(III) in synthesized nontronites in function of different Si species in solution, which in turn depend on pH.

In the same experiments performed by Pokrovski et al. (2003), they note that the presence of Si in the solution favors the formation of Fe-Si linkages. If we assume the hypothesis that the IRTOCM formation occurs similarly as suggested for other clay minerals first by the precipitation of octahedral sheet, followed by the formation of tetrahedral sheet (Carrado et al., 2000; Huertas et al., 2000), then M(II) and M(III) octahedral coordination in solution or polymerized hydroxide complexes would be determinant. However, as showed by Pokrovski et al. (2003) presence of aqueous Si inhibit Fe(III) polymerization and thus solid-phase formation. An earlier study on Si effect on Ga complexes (which can be considered similar to aluminium ones) shows similar trend, in the fact that in the presence of Si in solution Ga adopts tetrahedral coordination and Ga–Si complexes are formed Pokrovski et al. (2002). The formation of such complexes M(III)-Si in solution could then explain the facility to form homogenous gels, but difficulty to obtain crystalline structures as observed by de Kimpe et al. (1961) and Hem et al. (1973).

It has to be noted that the studies about element speciation in solution have been performed in diluted solutions and at ambient conditions, while the preparation of clay mineral precursors often is performed at concentrated solutions and the synthesis is carried out at hydrothermal conditions. In perspective, it would be interesting to investigate the element speciation and their synergistic effects at concentrated solutions and at elevated temperature and pressure.

8. Conclusion

Iron-rich tri-octahedral clay minerals have been identified occurring on the surface of Mars, in meteorites, deep-sea environment, subduction zones and transform faulting. The formation conditions of these clay minerals have not yet been fully understood. Moreover, the thermodynamic constants of these minerals are scarce, which does not allow to predict their stability in long term. This aspect is important for nuclear waste disposal sites, where the formation of iron-rich clay minerals have been observed on steel and clay-rich rock interface or at the interface between iron and silica glass. These minerals could also have a potential to be used as heterogeneous catalysts. In order to obtain sufficient amount of such minerals for further thermodynamic studies and to investigate their formation conditions, the synthesis of a series of iron-rich tri-octahedral clay minerals with different Si/Fe molar ratio is necessary. This study reviews the previously reported methods and conditions for iron-rich tri-octahedral clay mineral synthesis. Two different approaches have been used to hydrothermally synthesize iron-rich trioctahedral minerals : using gel or solid precursor. The synthesis of 1:1 type clay minerals were performed in reducing conditions in neutral or alkaline pH. The parameters for 2:1 type clay minerals synthesis was in most cases similar to 1:1 type clay mineral synthesis, but included also acidic pH and oxidizing conditions.

Previous synthesis of iron-rich tri-octahedral clay mineral phases have not been systematic, because the studies were focused on particular geological or application question. Therefore, in future, it could be interesting to investigate in the systematic manner the optimum synthesis conditions (nature and ratio of reactants, pH, temperature, time and water amount) starting from the simplest of the systems Si-Fe(II). The characterization of neoformed products should include powder X-ray diffraction, X-ray diffraction of oriented films (air-dried and saturated with ethylene glycol), FTIR and Mössbauer spectroscopies, as well as TEM.

In perspective, two areas of studies seem particularly interesting for further investigation: (1) the confrontation of experimental and geochemical simulation data, and (2) the effect of element speciation in solution on the chemical composition of the neoformed solid. Recently, a numerical simulation accounting for the processes of nucleation, growth, dissolution and ageing of particles in an initially supersaturated closed system was developed (Noguera et al., 2006a, b). It could then be interesting to observe the nucleation and crystal growth in Si-Fe system in real time in-situ and confront the obtained results with the simulations. The influence of a parameter such as the pH, its role on element speciation in solution and their subsequent effect on crystal growth and nucleation could be assessed.

Acknowledgments

We are grateful to two anonymous reviewers for their comments and suggestions, and Fabien Baron for his comments, suggestions and discussions, which have significantly improved the manuscript.

References

Andrieux, P., Petit, S., 2010. Hydrothermal synthesis of dioctahedral smectites: The Al-Fe3+ chemical series. Part I: Influence of experimental conditions. Appl. Clay Sci. 48, 5–17. https://doi.org/10.1016/j.clay.2009.11.019

Arundhathi, R., Sreedhar, B., Parthasarathy, G., 2011. Highly efficient heterogenous catalyst for O-arylation of phenols with aryl halides using natural ferrous chamosite. Appl. Clay Sci. 51, 131–137. https://doi.org/10.1016/j.clay.2010.11.014

Arundhathi, R., Sreedhar, B., Parthasarathy, G., 2010. Chamosite, a naturally occurring clay as a versatile catalyst for various organic transformations. Clay Miner. 45, 281–299. https://doi.org/10.1180/claymin.2010.045.3.281

Bailey, S.W., 1988. X-ray diffraction identification of the polytypes of mica, serpentine, and chlorite. Clays Clay Miner. 36, 193 LP-213.

Baker, L.L., Strawn, D.G., 2014. Temperature Effects on the Crystallinity of Synthetic Nontronite and Implications for Nontronite Formation in Columbia River Basalts. Clays Clay Miner. 62, 89 LP-101.

Baldermann, A., Dohrmann, R., Kaufhold, S., Nickel, C., Letofsky-Papst, I., Dietzel, M., 2014. The Fe-Mg-saponite solid solution series a hydrothermal synthesis study. Clay Miner. 49, 391–415. https://doi.org/10.1180/claymin.2014.049.3.04

Baldermann, A., Dohrmann, R., Kaufhold, S., Nickel, C., Letofsky-Papst, I., Dietzel, M., 2014. The Fe-Mg-saponite solid solution series – a hydrothermal synthesis study. Clay Miner. 49, 391–415.

Baldermann, A., Warr, L.N., Letofsky-Papst, I., Mavromatis, V., 2015. Substantial iron sequestration during green-clay authigenesis in modern deep-sea sediments. Nat. Geosci.

8, 3–8. https://doi.org/10.1038/ngeo2542

Baron, F., 2016. Thesis. Le fer dans les smectites : une approche par synthèses minérales. Université de Poitiers (France).

Baron, F., Petit, S., Tertre, E., Decarreau, A., 2016. Influence of Aqueous Si and Fe Speciation on Tetrahedral Fe(III) Substitutions in Nontronites: a Clay Synthesis Approach. Clays Clay Miner. 64, 230–244. https://doi.org/10.1346/CCMN.2016.0640309

Beaufort, D., Rigault, C., Billon, S., Billault, V., Inoue, A., Inoue, S., Patrier, P., 2015. Chlorite and chloritization processes through mixed-layer mineral series in low-temperature geological systems – a review. Clay Miner. 50, 497–523. https://doi.org/10.1180/claymin.2015.050.4.06

Bertoldi, C., Dachs, E., Cemic, L., Theye, T., Wirth, R., Groger, W., 2005. The Heat Capacity of the Serpentine Subgroup Mineral Berthierine (Fe2.5Al0.5)[Si1.5Al0.5O5](OH)4. Clays Clay Miner. 53, 380 LP-388.

Bethke, C.M., 2007. Geochemical and Biogeochemical Reaction Modeling. Cambridge University Press, Cambridge. https://doi.org/10.1017/CBO9780511619670

Blanc, P., Lassin, A., Piantone, P., Azaroual, M., Jacquemet, N., Fabbri, A., Gaucher, E.C., 2012. Thermoddem: A geochemical database focused on low temperature water/rock interactions and waste materials. Appl. Geochemistry 27, 2107–2116. https://doi.org/10.1016/j.apgeochem.2012.06.002

Boukili, B., El Moutaouakkil, N., Robert, J.-L., Meunier, A., Ventura, G.D., 2015. Experimental investigation of trioctahedral micas in the Na2O-FeO-Fe2O3-Al2O3-SiO2-H2O-HF system. J. Mater. Environ. Sci. 6, 2917–2928.

729 Bourg, I.C., 2015. Sealing Shales versus Brittle Shales: A Sharp Threshold in the Material
730 Properties and Energy Technology Uses of Fine-Grained Sedimentary Rocks. Environ.
731 Sci. Technol. Lett. 2, 255–259. https://doi.org/10.1021/acs.estlett.5b00233

732 Caillère, S., Henin, S., Esquevin, J., 1953. Synthèses à basse température de phyllite ferrifère.
733 Comptes Rendus l'Academie Sci. 237, 1724–1726.

734 Carrado, K.A., Decareau, A., Petit, S., Bergaya, F., Lagaly, G., 2006. Synthetic clay minerals
735 and purification of natural clays, in: Bergaya, F., Theng, B.K.G., Lagaly, G. (Eds.),
736 Handbook of Clay Science. Elsevier Ltd, 115–139. https://doi.org/10.1016/S1572-
737 4352(05)01004-4

738 Carrado, K.A., Xu, L., Gregory, D.M., Song, K., Seifert, S., Botto, R.E., 2000. Crystallization
739 of a layered silicate clay as monitored by small-angle X-ray scattering and NMR. Chem.
740 Mater. 12, 3052–3059. https://doi.org/10.1021/cm000366a

741 Chemtob, S.M., Nickerson, R.D., Morris, R. V., Agresti, D.G., Catalano, J.G., 2015. Synthesis
742 and structural characterization of ferrous trioctahedral smectites: Implications for clay
743 mineral genesis and detectability on Mars. J. Geophys. Res. Planets 120, 1119–1140.
744 https://doi.org/10.1002/2014JE004763

745 Chen, C.-H., 1975. A method of estimation of standard free energies of formation of silicate
746 minerals at 298.15 degrees K. Am. J. Sci. 275, 801–817.
747 https://doi.org/10.2475/ajs.275.7.801

748 Chermak, J.A., Rimstidt, J.D., 1989. Estimating the thermodynamic properties (Delta G of and
749 Delta H of) of silicate minerals at 298 K from the sum of polyhedral contributions. Am.
750 Mineral. 74, 1023–1031.

751 Chevrier, V., Poulet, F., Bibring, J., 2007. Early geochemical environment of Mars as

752 determined from thermodynamics of phyllosilicates. Nature 448, 2–5.
753 https://doi.org/10.1038/nature05961

754 de Combarieu, G., Barboux, P., Minet, Y., 2007. Iron corrosion in Callovo-Oxfordian argilite:
755 From experiments to thermodynamic/kinetic modelling. Phys. Chem. Earth 32, 346–358.
756 https://doi.org/10.1016/j.pce.2006.04.019

757 de Kimpe, C., Gastuche, M.C., Brindley, G.., 1961. Ionic coordination in alumino-silicic gels
758 in relation to clay mineral formation. Am. Mineral. 46, 1370–1381.

759 Decarreau, A., 1981. Cristallogenese à basse température de smectites trioctaèdriques par
760 vieillissement de coprécipités silicométalliques. Comptes rendus des séances l'Académie
761 des Sci. 292, 61–64.

762 Doelsch, E., Stone, W.E.E., Petit, S., Masion, A., 2001. Speciation and Crystal Chemistry of
763 Fe (III) Chloride Hydrolyzed in the Presence of SiO 4 Ligands . 2 . Characterization of
764 Si - Fe Aggregates by FTIR and 29 Si Solid-State NMR 1399–1405.

765 Dzene, L., 2016. Thesis. Influence of particle size and crystal chemistry on cation exchange
766 properties of swelling clay minerals. Université de Poitiers (France).

767 Eugster, H.P., Chou, I.-M., 1973. The Depositional Environments of Precambrian Banded Iron-
768 Formations. Econ. Geol. 68, 1144–1168.

769 Farmer, V.C., Krishnamurti, G.S.R., Htjang, A.P.M., 1991. Synthetic Allophane and Layer-
770 Silicate Formation in SiO2-A1203-FeO-Fe203-MgO-H20 Systems at 23 and 89 C in a
771 Calcareous Environment. Clays Clay Miner. 39, 561–570.

772 Feuillie, C., Daniel, I., Michot, L.J., Pedreira-Segade, U., 2013. Adsorption of nucleotides onto
773 Fe-Mg-Al rich swelling clays. Geochim. Cosmochim. Acta 120, 97–108.

https://doi.org/10.1016/j.gca.2013.06.021

Fialips, C.-I., Huo, D., Yan, L., Wu, J., Stucki, J.W., 2002. Effect of Fe oxidation state on the IR spectra of Garfield nontronite. Am. Mineral. 87, 630-641.

Fialips, C.I., Petit, S., Decarreau, A., Beaufort, D., 2000. Influence of synthesis pH on kaolinite "crystallinity" and surface properties. Clays Clay Miner. 48, 173–184. https://doi.org/10.1346/CCMN.2000.0480203

Flaschen, S.S., Osborn, E.F., 1957. Studies of the system iron oxide-silicawater at low oxygen partial pressures. Econ. Geol. 52, 923–943. https://doi.org/10.2113/gsecongeo.52.8.923

Frank-Kamenetzkij, V.A., Kotov, N. V, Tomashenko, A.N., 1973. The role of AlIV and AlVI in transformation and synthesis of layer silicates. Krist. und Tech. 8, 425–435. https://doi.org/10.1002/crat.19730080404

Garrido-Ramírez, E.G., Theng, B.K.G., Mora, M.L., 2010. Clays and oxide minerals as catalysts and nanocatalysts in Fenton-like reactions - A review. Appl. Clay Sci. 47, 182–192. https://doi.org/10.1016/j.clay.2009.11.044

Gates, W.P., 2008. Cation mass-valence sum (CM-VS) approach to assigning OH-bending bands in dioctahedral smectites. Clays Clay Miner. 56, 10–22. https://doi.org/10.1346/CCMN.2008.0560102

Grambow, B., 2016. Geological Disposal of Radioactive Waste in Clay. Elements 12, 239–245. https://doi.org/10.2113/gselements.12.4.239

Grauby, O., Petit, S., Decarreau, A., Baronnet, A., 1994. The nontronite-saponite series: an experimental approach. Eur. J. Mineral. 6, 99–112.

Grubb, P.L.C., 1971. Silicates and their paragenesis in the brockman iron formation of

796 Wittenoom Gorge, Western Australia. Econ. Geol. 66, 281–292.
797 https://doi.org/10.2113/gsecongeo.66.2.281

798 Halevy, I., Alesker, M., Schuster, E.M., Popovitz-Biro, R., Feldman, Y., 2017. A key role for
799 green rust in the Precambrian oceans and the genesis of iron formations. Nat. Geosci. 10,
800 135–139. https://doi.org/10.1038/ngeo2878

801 Hamilton, D.L., Henderson, C.M.B., 1968. The preparation of silicate compositions by a gelling
802 method. Mineral. Mag. 36, 832–838. https://doi.org/10.1180/minmag.1968.036.282.11

803 Harder, H., 1978. Synthesis of Iron Layer Silicate Minerals. Clays Clay Miner. 26, 65–72.
804 https://doi.org/10.1346/CCMN.1978.0260108

805 Helgeson, H.C., Delany, J.M., Nesbitt, H.W., Bird, D.K., 1978. Summary and Critique of the
806 Thermodynamic Properties of Rock-Forming Minerals. Yale University. Kline Geology
807 Laboratory.

808 Hem, J.D., Roberson, C.E., Lind, C.J., Polzer, W.L., 1973. Chemical Interactions of Aluminum
809 with Aqueous Silica at 25°C. Geological Survey Water-Supply Paper 1827-E.

810 Herbert, H.-J., Kasbohm, J., Nguyen-Thanh, L., Meyer, L., Hoang-Minh, T., Xie, M.,
811 Mählmann, R.F., 2016. Alteration of expandable clays by reaction with iron while being
812 percolated by high brine solutions. Appl. Clay Sci. 121–122, 174–187.
813 https://doi.org/10.1016/j.clay.2015.12.022

814 Holland, T.J.B., 1989. Dependence of entropy on volume for silicate and oxide minerals; a
815 review and predictive model. Am. Mineral. 74, 5–13.

816 Huertas, F.J., Cuadros, J., Huertas, F., Linares, J., 2000. Experimental study of the hydrothermal
817 formation of smectite in the Beidellite-Saponite series. Am. J. Sci.

https://doi.org/10.2475/ajs.300.6.504

Huve, L., 1992. Thesi. Synthèse de phyllosilicates en milieu acide et fluoré et leur caractérisation. Université de Haute-Alsace (France).

Inoué, S., Kogure, T., 2016. High-resolution transmission electron microscopy (HRTEM) study of stacking irregularity in fe-rich chlorite from selected hydrothermal ore deposits. Clays Clay Miner. 64, 131–144. https://doi.org/10.1346/CCMN.2016.0640205

Jaber, M., Komarneni, S., Zhou, C.-H., 2013. Synthesis of Clay Minerals, in: Bergaya, F., Lagaly, G. (Eds.), Handbook of Clay Science Fundamentals. Elsevier, pp. 223–241. https://doi.org/10.1016/B978-0-08-098258-8.00009-2

Johnson, J., Anderson, F., Parkhurst, D., 2000. Database thermo.com.V8.R6.230, Rev 1.11.

Kloprogge, J.T., Komarneni, S., Amonette, J.E., 1999. Synthesis of smectite clay minerals: A critical review. Clays Clay Miner. 47, 529–554. https://doi.org/10.1346/CCMN.1999.0470501

Kloprogge, J.T., Vogels, R.J.M.J., Van Der Eerden, A.M.J., 1996. Hydrothermal synthesis of pyrophyllite from Si-Al gels and salt solutions: Some implications for the formation of pyrophyllite in low-grade metamorphic rocks rich in aluminous smectites. Neues Jahrb. fur Mineral. Monatshefte 135–144.

Kodolányi, J., Pettke, T., Spandler, C., Kamber, B.S., Ling, K.G., 2012. Geochemistry of ocean floor and fore-arc serpentinites: Constraints on the ultramafic input to subduction zones. J. Petrol. 53, 235–270. https://doi.org/10.1093/petrology/egr058

Lanson, B., Lantenois, S., van Aken, P.A., Bauer, A., Plancon, A., 2012. Experimental investigation of smectite interaction with metal iron at 80 C: Structural characterization of

newly formed Fe-rich phyllosilicates. Am. Mineral. 97, 864–871. https://doi.org/10.2138/am.2012.4062

Lantenois, S., Lanson, B., Muller, F., Bauer, A., Jullien, M., Plançon, A., 2005. Experimental study of smectite interaction with metal Fe at low temperature: 1. Smectite destabilization. Clays Clay Miner. 53, 597–612. https://doi.org/10.1346/CCMN.2005.0530606

Le Pape, P., Rivard, C., Pelletier, M., Bihannic, I., Gley, R., Mathieu, S., Salsi, L., Migot, S., Barres, O., Villiéras, F., Michau, N., 2015. Action of a clay suspension on an Fe(0) surface under anoxic conditions: Characterization of neoformed minerals at the Fe(0)/solution and Fe(0)/atmosphere interfaces. Appl. Geochemistry 61, 62–71. https://doi.org/10.1016/j.apgeochem.2015.05.008

Li, H., Li, Y., Xiang, L., Huang, Q., Qiu, J., Zhang, H., Sivaiah, M.V., Baron, F., Barrault, J., Petit, S., Valange, S., 2015. Heterogeneous photo-Fenton decolorization of Orange II over Al-pillared Fe-smectite: Response surface approach, degradation pathway, and toxicity evaluation. J. Hazard. Mater. 287, 32–41. https://doi.org/10.1016/j.jhazmat.2015.01.023

McNaught, A.D., Wilkinson, A. (Eds.), 1997. IUPAC. Compendium of Chemical Terminology, 2nd ed. Blackwell Scientific Publishions, Oxford.

Meunier, A., Petit, S., Cockell, C.S., El Albani, A., Beaufort, D., 2010. The Fe-rich clay microsystems in basalt-komatiite lavas: Importance of Fe-Smectites for Pre-Biotic molecule catalysis during the Hadean eon. Orig. Life Evol. Biosph. 40, 253–272. https://doi.org/10.1007/s11084-010-9205-2

Miyawaki, R., Tomura, S., Samejima, S., Okazaki, M., Misuta, H., Maruyama, S., Shibasaki, Y., 1991. Effects of Solution Chemistry on the Hydrothermal Synthesis of Kaolinite. Clays Clay Miner. 39, 498–508. https://doi.org/10.1346/CCMN.1991.0390505

Mizutani, T., Fukushima, Y., Okada, A., Kamigaito, O., Kobayashi, T., 1991. Synthesis of 1:1 and 2:1 Iron Phyllosilicates and Characterization of their Iron State by Mössbauer Spectroscopy. Clays Clay Miner. 39, 381–386. https://doi.org/10.1346/CCMN.1991.0390407

Mosser-Ruck, R., Cathelineau, M., Guillaume, D., Charpentier, D., Rousset, D., Barres, O., Michau, N., 2010. Effects of Temperature, pH, and Iron/Clay and Liquid/Clay Ratios on Experimental Conversion of Dioctahedaral Smectite to Berthierine, Chlorite, Vermiculite, or Saponite. Clays Clay Miner. 58, 280–291. https://doi.org/10.1346/CCMN.2010.0580212

Mosser-Ruck, R., Pignatelli, I., Bourdelle, F., Abdelmoula, M., Barres, O., Guillaume, D., Charpentier, D., Rousset, D., Cathelineau, M., Michau, N., 2016. Contribution of long-term hydrothermal experiments for understanding the smectite-to-chlorite conversion in geological environments. Contrib. to Mineral. Petrol. 171, 1–21. https://doi.org/10.1007/s00410-016-1307-z

Neumann, A., Sander, M., Hofstetter, T.B., 2011. Redox Properties of Structural Fe in Smectite Clay Minerals BT - Aquatic Redox Chemistry. Aquat. Redox Chem. 1071, 361–379.

Noguera, C., Fritz, B., Clément, A., Baronnet, A., 2006a. Nucleation, growth and ageing scenarios in closed systems I: A unified mathematical framework for precipitation, condensation and crystallization. J. Cryst. Growth 297, 180–186. https://doi.org/10.1016/j.jcrysgro.2006.08.049

Noguera, C., Fritz, B., Clément, A., Baronnet, A., 2006b. Nucleation, growth and ageing scenarios in closed systems II: Dynamics of a new phase formation. J. Cryst. Growth 297, 187–198. https://doi.org/10.1016/j.jcrysgro.2006.08.048

886 Nriagu, J.O., 1975. Thermochemical approximations for clay minerals. Am. Mineral. 60, 834–
887 839.

888 Osacký, M., Šucha, V., Czímerová, A., Pentrák, M., Madejová, J., 2013. Reaction of smectites
889 with iron in aerobic conditions at 75°C. Appl. Clay Sci. 72, 26–36.
890 https://doi.org/10.1016/j.clay.2012.12.010

891 Parkhurst, D.L., Appelo, C.A.J., 2013. Description of input and examples for PHREEQC
892 version 3 - A computer program for speciation, batch-reaction, one-dimensional transport
893 and inverse geochemical calculations.

894 Pedreira-Segade, U., Feuillie, C., Pelletier, M., Michot, L.J., Daniel, I., 2016. Adsorption of
895 nucleotides onto ferromagnesian phyllosilicates: Significance for the origin of life.
896 Geochim. Cosmochim. Acta 176, 81–95. https://doi.org/10.1016/j.gca.2015.12.025

897 Peretyazhko, T.S., Sutter, B., Morris, R. V., Agresti, D.G., Le, L., Ming, D.W., 2016. Fe/Mg
898 smectite formation under acidic conditions on early Mars. Geochim. Cosmochim. Acta
899 173, 37–49. https://doi.org/10.1016/j.gca.2015.10.012

900 Petit, S., Baron, F., Decarreau, A., 2017. Synthesis of nontronite and other Fe-rich smectites : a
901 critical review. Clay Miner. 52, 469–483. https://doi.org/10.1180/claymin.2017.052.4.05

902 Pignatelli, I., Bourdelle, F., Bartier, D., Mosser-Ruck, R., Truche, L., Mugnaioli, E., Michau,
903 N., 2014. Iron-clay interactions: Detailed study of the mineralogical transformation of
904 claystone with emphasis on the formation of iron-rich T-O phyllosilicates in a step-by-step
905 cooling experiment from 90°C to 40°C. Chem. Geol. 387, 1–11.
906 https://doi.org/10.1016/j.chemgeo.2014.08.010

907 Pignatelli, I., Mugnaioli, E., Hybler, J., Mosser-Ruck, R., Cathelineau, M., Michau, N., 2013.
908 A multi-technique characterization of cronstedtite synthesized by iron-clay interaction in

a step-by-step cooling procedure. Clays Clay Miner. 61, 277–289. https://doi.org/10.1346/CCMN.2013.0610408

Pokrovski, G.S., Schott, J., Farges, F., Hazemann, J.L., 2003. Iron (III)-silica interactions in aqueous solution: Insights from X-ray absorption fine structure spectroscopy. Geochim. Cosmochim. Acta 67, 3559–3573. https://doi.org/10.1016/S0016-7037(03)00160-1

Pokrovski, G.S., Schott, J., Hazemann, J., Farges, F., Pokrovsky, Oleg, S., 2002. An X-ray absorption fine structure and nuclear magnetic resonance spectroscopy study of gallium–silica complexes in aqueous solution. Geoch Cosmochim. Acta 66, 4203–4322.

Reynolds, R.C., DiStefano, M.P., Lahann, R.W., 1992. Randomly interstratified serpentine/chlorite; its detection and quantification by powder X-ray diffraction methods. Clays Clay Miner. 40, 262 LP-267.

Rivard, C., Montargès-Pelletier, E., Vantelon, D., Pelletier, M., Karunakaran, C., Michot, L.J., Villieras, F., Michau, N., 2013. Combination of multi-scale and multi-edge X-ray spectroscopy for investigating the products obtained from the interaction between kaolinite and metallic iron in anoxic conditions at 90 °C. Phys. Chem. Miner. 40, 115–132. https://doi.org/10.1007/s00269-012-0552-6

Rivard, C., Pelletier, M., Michau, N., Razafitianamaharavo, A., Abdelmoula, M., Ghanbaja, J., Villiéras, F., 2015. Reactivity of callovo-oxfordian claystone and its clay fraction with metallic Iron: Role of non-clay minerals in the interaction mechanism. Clays Clay Miner. 63, 290–310. https://doi.org/10.1346/CCMN.2015.0630404

Roy, D.M., Roy, R., 1954. An experimental study of the formation and properties of synthetic serpentines and related layer silicate minerals. Am. Mineral. 53, 957–975.

Snow, C.L., Lee, C.R., Shi, Q., Boerio-Goates, J., Woodfield, B.F., 2010a. Size-dependence of

the heat capacity and thermodynamic properties of hematite (α-fe2o3). J. Chem. Thermodyn. 42, 1142–1151. https://doi.org/10.1016/j.jct.2010.04.009

Snow, C.L., Shi, Q., Boerio-Goates, J., Woodfield, B.F., 2010b. Heat Capacity Studies of Nanocrystalline Magnetite (Fe_3O_4). J. Phys. Chem. C 114, 21100–21108. https://doi.org/10.1021/jp1072704

Snow, C.L., Smith, S.J., Lang, B.E., Shi, Q., Boerio-Goates, J., Woodfield, B.F., Navrotsky, A., 2011. Heat capacity studies of the iron oxyhydroxides akaganéite (β-FeOOH) and lepidocrocite (γ-FeOOH). J. Chem. Thermodyn. 43, 190–199. https://doi.org/10.1016/j.jct.2010.08.022

Sposito, G., 1986. The polymer model of thermochemical clay mineral stability. Clays Clay Miner. 34, 198–203. https://doi.org/10.1346/CCMN.1986.0340210

Sreedhar, B., Arundhathi, R., Reddy, M.A., Parthasarathy, G., 2009. Highly efficient heterogenous catalyst for acylation of alcohols and amines using natural ferrous chamosite. Appl. Clay Sci. 43, 425–434. https://doi.org/10.1016/j.clay.2008.10.001

Stølen, S., Glöckner, R., Grønvold, F., Atake, T., Izumisawa, S., 1996. Heat capacity and thermodynamic properties of nearly stoichiometric wüstite from 13 to 450 K. Am. Mineral. 81, 973–981. https://doi.org/10.2138/am-1996-7-819

Stucki, J.W., 2013. Properties and Behaviour of Iron in Clay Minerals, in: Bergaya, F., Lagaly, G. (Eds.), Handbook of Clay Science Fundamentals. Elsevier, pp. 559–611. https://doi.org/10.1016/B978-0-08-098258-8.00018-3

Stucki, J.W., Goodman, B.A., Schwertmann, U. (Eds.), 1989. Iron in Soils and Clay Minerals, Soil Science. D. Reidel Publishing Company. https://doi.org/10.1097/00010694-198904000-00013

955 Tardy, Y., Fritz, B., 1981. An ideal solid solution model for calculating solubility of clay
956 minerals. Clay Miner. 361–373.

957 Tardy, Y., Garrels, R.M., 1974. A method of estimating the Gibbs energies of formation of
958 layer silicates. Geochim. Cosmochim. Acta 38, 1101–1116. https://doi.org/10.1016/0144-
959 2449(86)90007-2

960 Tosca, N.J., Guggenheim, S., Pufahl, P.K., 2016. An authigenic origin for Precambrian
961 greenalite: Implications for iron formation and the chemistry of ancient seawater. Geol.
962 Soc. Am. Bull. 128, 511–530. https://doi.org/10.1130/B31339.1

963 Trujillano, R., Rico, E., Vicente, M.A., Rives, V., Chaabene, B.E.N., Ghorbel, A., 2009.
964 Microwave-Assisted Synthesis of Fe3+ Saponites. Characterization by X-Ray Diffraction
965 and FT-IR Spectroscopy. Rev. la Soc. española Mineral. 11, 189–190.

966 Van Hise, C.R., Leith, C.K., 1911. Precipitation of greenalite, in: The Geology of Lake Superior
967 Region. U.S. Geological Survey, Washington, 521–525.

968 Vieillard, P., 2000. A new method for the prediction of Gibbs free energies of formation of
969 hydrated clay minerals based on the electronegativity scale. Clays Clay Miner. 48, 459–
970 473. https://doi.org/10.1346/CCMN.2000.0480406

971 Vieillard, P., 1994. Prediction of enthalpy of formation based on refined crystal structures of
972 multisite compounds: Part 1. Theories and examples. Geochim. Cosmochim. Acta 58,
973 4049–4063. https://doi.org/10.1016/0016-7037(94)90266-6

974 Wang, X., Dong, H., Zeng, Q., Xia, Q., Zhang, L., Zhou, Z., 2017. Reduced Iron-Containing
975 Clay Minerals as Antibacterial Agents. Environ. Sci. Technol. 51, 7639–7647.
976 https://doi.org/10.1021/acs.est.7b00726

977 Wilkins, R.W.T., Ito, J., 1967. Infrared Spectra of Some Synthetic Talcs. Am. Mineral. 52,
978 1649–1661.

979 Wilson, J.C., Benbow, S., Sasamoto, H., Savage, D., Watson, C., 2015. Thermodynamic and
980 fully-coupled reactive transport models of a steel–bentonite interface. Appl. Geochemistry
981 61, 10–28. https://doi.org/10.1016/j.apgeochem.2015.05.005

982 Zhang, D., Zhou, C.-H., Lin, C.-X., Tong, D.-S., Yu, W.-H., 2010. Synthesis of clay minerals.
983 Appl. Clay Sci. 50, 1–11. https://doi.org/10.1016/j.clay.2010.06.019

984 Zolotov, M.Y., 2015. Formation of brucite and cronstedtite-bearing mineral assemblages on
985 Ceres. Icarus 228, 13–26. https://doi.org/10.1016/j.icarus.2013.09.020